Journal of the Serbian Chemical Society
JSCS-info@shd.org.rs • www.shd.org.rs/JSCS
J. Serb. Chem. Soc. *85* (2) 215–225 (2020)
JSCS–5295
UDC 542.9+547.571'551+546.732'562:519.677:615.28
Original scientific paper

Synthesis, characterization, thermal, theoretical and antimicrobial studies of Schiff base ligand and its Co(II) and Cu(II) complexes

RADHA VENKITTAPURAM PALANISWAMY[1], MAHALAKSHMI DHANDAPANI[2], JONEKIRUBAVATHY SUYAMBULINGAM[2] and CHITRA SUBRAMANIAN[2]*

[1]*Department of Chemistry, Jansons Institute of Technology, Coimbatore 641659, Tamil Nadu, India and* [2]*Department of Chemistry, P.S.G.R. Krishnammal College for Women, Coimbatore 641004 Tamil Nadu, India*

(Received 28 November 2018, revised 21 May, accepted 24 May 2019)

Abstract: A Schiff base ligand **L** was synthesized by condensation of 1,2-diaminoethane with creatinine. The reaction of the ligand with metal chloride salt gives Co(II) and Cu(II) complexes. The synthesized ligand and its metal complexes were characterized by elemental analysis, FT-IR, NMR, UV–Vis, conductivity and magnetic susceptibility measurements as well as thermal analyses. Based on spectral data, tetrahedral geometries have been proposed for the Co(II) and Cu(II) complexes. The molar conductivity data show that the complexes are non-electrolytic in nature. In DFT studies, the geometry of the Schiff base ligand and its Co(II) and Cu(II) complexes were fully optimized using the B3LYP functional together with 6-31g(d,p) and LANL2DZ basis sets. The ligand and its metal complexes were tested against four bacterial species and two fungal species. The results revealed that the metal complexes are more potent against the microbes than the parent ligand.

Keywords: Schiff base; Co(II), Cu(II); DFT; biological.

INTRODUCTION

Transition metal complexes with organic ligands have been the premise of concentrated research due to their role as contrasting agents, radiopharmaceuticals and chemotherapeutics in the treatment of metal toxicity.[1] Schiff bases are interesting class of compounds in coordination chemistry[2] and are called as privileged ligands due to their facile synthetic approaches by condensing an aldehyde or ketone with amines. These ligands easily stabilize different metals in various oxidation states.[3] Schiff bases and their transition metal complexes show a wide range of applications in industrial,[4] pharmaceutical[5,6] and chemical fields.[7,8]

* Corresponding author. E-mail: rajshree1995@rediffmail.com
https://doi.org/10.2298/JSC181128049V

They also exhibit biological activities, such as antitumor, anti-bacterial, fungicidal, anticarcinogenic[9–13] and antioxidant activities.[14,15]

A number of substituted imidazoles are active in inflammation, neurodegenerative diseases and tumours of the nervous system.[16,17] Synthetic imidazoles are present in many fungicides and antifungal, antiprotozoal and antihypertensive medications. In view of the above findings, an imidazole pharmacophore was incorporated in the synthesis of a Schiff base ligand. Herein the synthesis of a Schiff base ligand and its Co(II) and Cu(II) complexes are reported. The prepared ligand was characterized by FT-IR, ^{1}H-NMR, ^{13}C-NMR and UV–Vis, in addition to elemental analysis and the complexes were characterized by FT-IR, UV–-Vis, elemental analysis, molar conductivity and magnetic susceptibility. The structure of the ligand and its metal complexes were optimized by DFT methods. The antimicrobial activity of the ligand and the complexes were tested against various microorganisms.

EXPERIMENTAL

Materials and methods

All the chemicals and the solvents were purchased from Sigma-Aldrich or Hi media Ltd. and used without further purification. The FT-IR spectra were recorded in the range 4000–400 cm^{-1} on Shimadzu IR affinity 1 spectrophotometer. The electronic spectra of the ligand and the complexes were recorded in the range 200–800 nm at room temperature in the solid state using a Shimadzu model UV-1601 spectrophotometer. Microanalyses (C, H and N) of the ligand and their complexes were recorded on an Elementar Vario EL III CHN analyser. Melting points of the compounds were determined in open capillaries in an electrical melting point apparatus. The NMR spectra of the ligand was recorded in DMSO-d_6 using a Bruker Avance III 400 MHz FT-digital NMR spectrometer. The magnetic moments of the complexes were determined on a Guoy balance and the diamagnetic corrections of the complexes were calculated using Pascal's constants. Molar conductivities of the complexes were measured in DMSO solution at 10^{-3} M concentration. The metal contents were estimated with a standard ethylenediaminetetraacetic acid solution. Thermogravimetric analysis of the complexes was performed from room temperature to 800 °C using a Perkin Elmer STA 6000 thermal analyser.

Synthesis of ligand

A mixture of a hot ethanolic solution of 1,2-diaminoethane (1 mmol in 10 mL) and creatinine (2-imino-1-methylimidazolidin-4-one, 2 mmol) was refluxed with stirring for 6 h. The reaction mass was concentrated on a rotary evaporator, over a water bath. The obtained Schiff base was filtered, washed with cold ethanol, dried and recrystallised from ethanol. Characterisation data for the ligand are given in the Supplementary material to this paper

Synthesis of metal complexes

A methanolic solution of metal chloride, $CoCl_2 \cdot 6H_2O$ or $CuCl_2 \cdot 2H_2O$ (1 mmol in 25 mL) was added dropwise to a magnetically stirred solution of ligand (1 mmol) dissolved in 15 mL of methanol. The stirring was continued for 2 h. The solid complex separated out and was filtered, washed with methanol and dried under vacuum. The synthetic procedure for the

Schiff base and its metal complexes are shown in (Scheme 1). Characterisation data for the complexes are given in the Supplementary material to this paper.

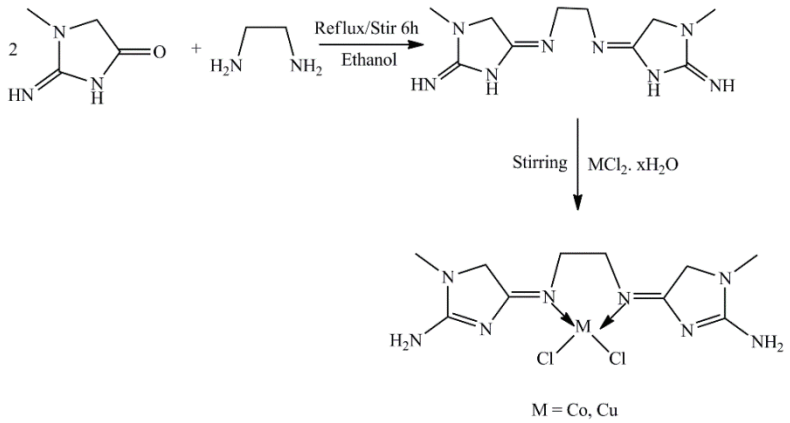

Scheme 1. Synthesis of Schiff base ligand and its metal complexes.

DFT studies

Theoretical calculations of the ligand and complexes were conducted using the density function theory (DFT)[18,19] using the B3LYP functional together with the 6-31G(d,p) and LANL2DZ basis sets.[20,21] Geometry optimization, molecular energy, dipole moments, natural bond orbital (NBO), nonlinear optical (NLO) properties and molecular electrostatic potential calculations were calculated at the same level with the 6-31G(d,p) basis set as incorporated in the Gaussian 09 program.[22,23]

Antimicrobial activity

The newly synthesized Schiff base ligand and its metal complexes were screened for their antimicrobial activities by the well dilution method.[24] The *in vitro* antibacterial activity of the test compounds was tested against two Gram-positive bacterial strains, *Staphylococcus aureus* (25923) and *Bacillus subtilis* (6051), and two Gram-negative bacterial strains, *Escherichia coli* (25922) and *Pseudomonas aeruginosa* (15422). The *in vitro* antifungal activities were realized against two fungal strains, *Aspergillus niger* (10231) and *Candida albicans* (6275).

RESULTS AND DISCUSSION

The newly synthesized Schiff base ligand and its metal complexes are coloured solids and stable at room temperature. The complexes have high melting points (> 250 °C). The Schiff base ligand is soluble in common organic solvents, such as methanol, ethanol, *etc*., whereas the complexes are soluble in DMF and DMSO. The elemental analysis and analytical data suggest that the metal to ligand ratio of the complexes is 1:1 stoichiometry of the type $[M(L)Cl_2]$.

FT-IR spectroscopy

The prominent modes of bonding in the Schiff base ligand **L** and its complexes were investigated by a comparative study of the FT-IR spectral data

(Table S-I of the Supplementary material). The IR spectrum of the Schiff base ligand **L** (Fig. S-1 of the Supplementary material) shows a strong band at 1690 cm^{-1}, which was assigned to the azomethine, ν(>C=N), group. The FT-IR spectra of the complexes **1** and **2** showed bands at around 1641 and 1628 cm^{-1} exhibiting a downward shift, which is in accordance with the coordination of the azomethine nitrogen to the metal ions.[25] This was further confirmed by the appearance of bands at around 418 and 434 cm^{-1}, corresponding to the ν(M–N) stretching vibration.[26] The ligand exhibits medium intensity bands at around 1560 and 3277 cm^{-1}, corresponding to the ν(C=NH) and ring >NH groups. The metal complexes showed bands at around 3347, 3186 cm^{-1} and 3362, 3156 cm^{-1} corresponding to NH_2 group. The disappearance of bands corresponding to ν(C=NH) and ring >NH vibrations and the appearance of bands corresponding to NH_2 vibrations in the metal complexes indicates the existence of amino–imino tautomerism. The appearance of bands around 369 and 371 cm^{-1} could be attributed to ν(M–Cl) stretching of the complexes.[9]

Molar conductance

The molar conductance of the newly synthesized complexes was measured at room temperature. The Co(II) and Cu(II) complexes have molar conductivity values of 15 and 22 Ω^{-1} cm^2 mol^{-1}, respectively. These data suggest that the complexes are non-electrolytic in nature.[27]

^{1}H-NMR spectrum

The ^{1}H-NMR spectrum of the Schiff base ligand **L** (Fig. S-2 of the Supplementary material) shows signals at δ 3.3 and 3.6 ppm, corresponding to CH_2 protons of the five-membered ring and ethane. The signal at δ 2.9 ppm was assigned to CH_3 protons. The singlet at δ 9.8 ppm corresponds to the NH proton of the creatinine moiety.

^{13}C-NMR spectrum

The signal corresponding to the imine carbon atom (C=N) of the ligand **L** is observed at δ 172.01 ppm. The signals corresponding to the methyl carbon of the heterocyclic ring is observed at δ 39.99 ppm and the CH_2 carbon of the heterocyclic ring at δ 56.66 ppm. The signal corresponding to the C=NH carbon is observed at δ 185.27 ppm. The signal corresponding to the CH_2 carbon of ethane is observed at δ 31.17 ppm The ^{13}C-NMR spectrum of the ligand **L** is shown in (Fig. S-3).

UV–Vis spectra and magnetic moment

The electronic spectral data and the magnetic moments reveal information regarding the geometry of the metal complexes. The UV–Vis spectra of the ligand and the metal complexes (Fig. S-4a) were recorded in the solid state at room

temperature and the data are shown in Table S-II of the Supplementary material. The electronic spectra of the ligand exhibited two characteristic bands at 235 and 350 nm corresponding to π→π* and n→π* transitions, respectively.[28] The Co(II) complex **1** showed two bands at 620 and 581 nm, which may be assigned to $^4T_1(F)\leftarrow{}^4A_2$ and $^4T_1(P)\leftarrow{}^4A_2$ transitions, indicating tetrahedral geometry.[29,30] The magnetic moment value of 4.25 μ_B also confirmed the tetrahedral geometry[30] of the Co(II) complex **1**. The Cu(II) complex **2** showed a broad band at around 850–950 nm corresponding to a d–d transition, indicating the tetrahedral geometry.[32,33] The magnetic moment value of 1.93 μ_B also supports the tetrahedral geometry[34] of the Cu(II) complex **2**.

Thermogravimetric analysis

The thermogravimetric and differential thermal analysis of Co(II) and Cu(II) complexes were realized from room temperature to 800 °C to study the thermal stability of the complexes. The stepwise thermal degradation of the complexes is depicted in Table I.

TABLE I. Thermogravimetric data of the ligand and its complexes

Complex	Decomposition temperature, °C	Weight loss, %		Content of metal oxide, %		Inference
		Obsd.	Calcd.	Obsd.	Calcd.	
$[Co(L)Cl_2]$ (**1**)	262	32.49	33.38	–	–	Loss due to $Cl_2+C_2H_4N_2$
	357	46.33	51.02	–	–	Loss due to $C_8H_{14}N_6$
	717			21.18	19.71	Loss due to organic moiety.
$[Cu(L)Cl_2]$ (**2**)	299	17.54	18.43	–	–	Loss of Cl_2
	605	58.26	65.75	–	–	Loss due to $C_{10}H_{18}N_8$
				21.20	20.67	Loss due to organic moiety.

The thermogram of Co(II) complex **1** (Fig. S-5) shows three decomposition steps. The first two decomposition steps within the temperature range 200–485 °C corresponds to loss of chlorine atoms and the organic moiety of the ligand with mass loss of 32.49 % (calcd. 33.38 %). The final decomposition within the temperature range 485–760 °C corresponds to loss of the creatinine moiety with a weight loss of 46.33 % (calcd. 51.02 %) leaving CoO as the final decomposition product.

The thermogram of Cu(II) complex **2** (Fig. S-6) represents decomposition in two steps. The decomposition step in the range 160–300 °C corresponds to loss of chlorine atoms with a mass loss of 17.54 % (calcd. 18.43 %). The second decomposition step in the range 300–658 °C with an estimated mass loss of 58.26

% (calcd. 65.75 %) may be attributed to loss of organic moieties of the ligand leaving CuO behind as the decomposition product.

Computational studies

Geometry optimization and electronic structure. The ground state geometry optimization for the ligand **L** and its Co(II) and Cu(II) complexes were performed in the gas phase using the B3LYP functional together with the LANL2DZ and 6-31G(d,p) basis sets as incorporated in the Gaussian 09W program. The optimized geometry of the ligand and its Co(II) and Cu(II) complexes are shown in Fig. 1. The C_6–N_4, C_3–N_3 bond lengths of the Schiff base ligand **L**, Co(II) complex **1** and Cu(II) complex **2** were found to be 1.273, 1.274, 1.303, 1.303 and 1.304 and 1.304 Å, respectively. The slight increase in bond length of the complexes confirms the coordination of ligand to the metal ion through the azomethine nitrogen. The slight elongation of C_2–N_8 and C_8–N_7 bonds of the complexes from 1.278 to 1.359 Å corresponds to the change of double to single bond in both the complexes. A decrease in the bond length was observed for the C_2–N_2 and C_8–N_6 bonds from 1.403 to 1.341 Å in the complex compared with the ligand confirming the amino–imino tautomerism of the creatinine moiety. The ligand shows an absorption band at around 235 nm corresponding to $\pi \rightarrow \pi^*$ transition. This assignment was supported by TDDFT calculations. The Co(II) complex shows two bands at around 620 and 581 nm corresponding to $^4T_1(F) \leftarrow {}^4A_2$ and $^4T_1(P) \leftarrow {}^4A_2$ transitions. The TDDFT calculations also showed two bands at 830 and 596 nm supporting the experimental data. The Cu(II) complex shows a broad d–d transition at around 850–950 nm. The TDDFT calculations also showed a band at around 996 nm supporting the experimental data (Fig. S-4b).

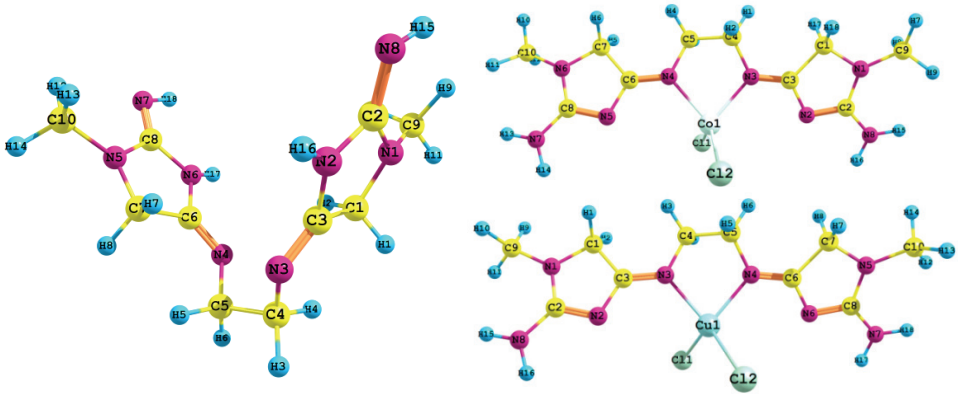

Fig. 1. Optimized geometry of the ligand **L**, and the Co(II) and Cu(II) complexes.

Frontier molecular orbitals

The frontier molecular orbitals (HOMO and LUMO) contribute to the stability or reactivity of compounds. The activity, stability and excitability of compounds can be studied by the energy difference of HOMO and LUMO.[35] The higher the energy difference is, the greater is the stability of the compound. The HOMO of the ligand is located on one of the imidazoline moiety, whereas the LUMO is located on the two azomethine groups and imidazoline moieties. The HOMO and LUMO energy difference of ligand **L** was found to be 6.1775 eV, indicating the good stability of the ligand. The Koopmans theorem[36] was used to calculate various chemical reactivity parameters which are tabulated in Table S-III.

Molecular electrostatic potential

The molecular electrostatic potential can be used for describing the structural properties of a molecule, such as chemical reactivity and dipole moment. The MEP map of ligand L was calculated at the same level of theory and is shown in Fig. 2. The negative regions, shown by the red colour, were located on the azomethine nitrogen atoms. The electron deficient regions (positive region), indicated by the blue colour, were located on the hydrogen atoms. According to the figure, the nitrogen atoms have negative charge while hydrogen atoms have a positive charge. Hence, the azomethine nitrogen atom coordinates to the metal atoms in complex formation.

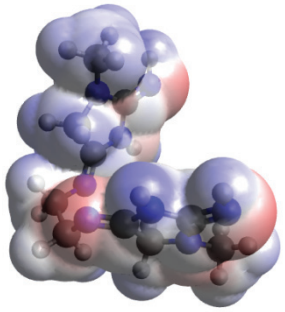

Fig. 2 Molecular electrostatic potential of the Schiff base ligand L.

Nonlinear optical properties

The dipole moment, linear polarizability and first-order hyperpolarizability of the ligand were calculated at the B3LYP functional with the 6-31G(d,p) basis set using the Gaussian 09W program. The polarizability and hyperpolarizability tensors are obtained by the job output file of Gaussian. The mean polarizability (α_{tot}), anisotropy of polarizability ($\Delta\alpha$) and the average of the first order hyperpolarizability (β_{tot}) were calculated. The calculated values are listed in Table S--IV. The values of α_{tot} and β_{tot} for the ligand are –107.78 a.u and 7.17026×10^{-31} esu, which are greater than the values for urea (α_{tot} and β_{tot} of urea are –21.5925

a.u and 1.3729×10^{-31} esu calculated at the same level). The β_{tot} value of the ligand is 5 times larger than that of urea. These results reveal that the Schiff base ligand could be a candidate as a NLO material.

Biological studies

The synthesized Schiff base ligand **L** and its Co(II) and Cu(II) complexes **1** and **2** were screened for their antimicrobial activity against two Gram positive bacteria, *Staphylococcus aureus* and *Bacillus subtilis*, two Gram negative bacteria, *Escherichia coli* and *Pseudomonas aeruginosa*, and two fungi, *Aspergillus niger* and *Candida albicans.* The diameter of the zone of inhibition (mm) was used to compare the antimicrobial activity with the standards ciprofloxacin and clotrimazole and the results are presented in Table S-V and Figs. S-7 and S-8.

The results revealed that the metal complexes exhibit enhanced activity against all the microbes compared to the ligand. The metal complex **1** showed sound activity against *E. coli* and *P. aeruginosa* with a zone diameter of 33 and 37 mm, respectively, which are close to that of the standards, whereas complex **2** also showed better activity than the ligand, with a zone diameter of 25 and 17 mm against the same microbes. The metal complexes **1** and **2** exhibited inhibition against *C. albicans* and *A. niger* with zone diameter of 26, 28 and 27 mm, 9 mm, respectively. The metal complexes **1** and **2** showed a large zone of inhibition against *S. aureus* and *B. subtilis* with zone diameters of 29, 29 and 20 mm, 18mm, respectively.

The minimum inhibitory, *MIC*, values of the Co(II) complex **1** against *B. subtilis*, *E. coli* and *C. albicans* are given in Table II. It is clear from the data that complex **1** (*MIC* 31.25 μg mL^{-1}) exhibits good activity against *C. albicans* compared to *MIC* 125 μg mL^{-1} against *B. subtilis* and *E. coli.* From these data it could be concluded that the metal complexes exhibit better activity against the tested microorganisms than the ligand.

TABLE II. Minimum inhibitory concentration (*MIC*) of $[CoLCl_2]$ (**1**)

S. No	Organism	Concentration of ligand **1**, μg mL^{-1}						
		1000	500	250	125	62.5	31.25	15.625
1.	*B. subtilis*	–	–	–	–	+	+	+
2.	*E. coli*	–	–	–	–	+	+	+
3.	*C. albicans*	–	–	–	–	–	–	+

The enhanced activity of the metal complexes could be explained based on the Tweedy chelation theory.[37] The chelation reduces the polarity of metal ions due to partial sharing of its positive charge with heteroatoms of the ligand. The reduction in polarity enhances the lipophilic nature of the chelates forming an interface between the lipid and the metal ion that can subsequently cross the permeability barrier of the cell. This leads to blockage of metal binding sites in

the enzymes of the microorganisms. The metal chelators perturb the respiration of the cell and reduce the synthesis of proteins, which inhibits the growth of the microorganisms. Apart from chelation, various other factors, such as size, solubility, dipole moment, concentration and hydrophobicity, have substantial influence on the antimicrobial activity, so that enhanced antimicrobial activity of the metal complexes may not be only due to chelation, but also to various other factors.[38–41]

CONCLUSIONS

A novel Schiff base ligand and its Co(II) and Cu(II) complexes were synthesized and characterized by various spectroscopic and analytical techniques. These data suggested a tetrahedral geometry for the Co(II) and Cu(II) complexes with 1:1 (metal:ligand) stoichiometry. The thermal stability of the complexes was studied by TGA/DTA analysis. The structures of the ligand and its metal complexes were optimized by DFT methods. In addition, *in vitro* antimicrobial activities of the ligand and the metal complexes were determined, which revealed that the metal complexes were more potent against the microorganisms.

SUPPLEMENTARY MATERIAL

Analytical and spectral data, as well as additional experimental data, are available electronically from http://www.shd.org.rs/JSCS/, or from the corresponding author on request.

ИЗВОД

СИНТЕЗА, КАРАКТЕРИЗАЦИЈА, ТЕРМАЛНА И АНТИМИКРОБНА ИСПИТИВАЊА КОМПЛЕКСА КОБАЛТА(II) И БАКРА(II) СА ШИФОВОМ БАЗОМ КАО ЛИГАНДОМ

RADHA VENKITTAPURAM PALANISWAMY[1], MAHALAKSHMI DHANDAPANI[2], JONEKIRUBAVATHY SUYAMBULINGAM[2] и CHITRA SUBRAMANIAN[2]

[1]*Department of Chemistry, Jansons Institute of Technology, Coimbatore 641659, Tamil Nadu, India* и [2]*Department of Chemistry, P.S.G.R. Krishnammal College for Women, Coimbatore 641004 Tamil Nadu, India*

Кондензационом реакцијом између 1,2-диаминоетана и креатинина синтетисан је лиганд (**L**) типа Шифове базе. Полазећи од $CuCl_2$ и $CoCl_2$ и лиганда **L** синтетисани су одговарајући комплекси ових јона метала. Синтетисани комплекси су окарактерисани на основу резултата елементалне микроанализе, FT-IR, NMR и UV–Vis спектроскопије, термалне анализе и магнетних мерења. На основу спектроскопских мерења закључено је да комплекси Co(II) и Cu(II) имају тетраедарску геометрију. Резултати кондуктометријских испитивања су показали да су синтетисани комплекси неелектролити. Оптимизација геометрије лиганда и одговрајућих комплекса извршена је DFT методом применом B3LYP функционала, као и 6-31g(d,p) и LANL2DZ базичних сетова. Антимикробна својства лиганда и комплекса Co(II) и Cu(II) испитивана су на различитим сојевима бактерија и гљива. Резултати ових испитивања су показали да су наведени комплекси значајно активнији у односу на одговарајући лиганд.

(Примљено 28 новембра 2018, ревидирано 21. маја, прихваћено 24. маја 2019)

REFERENCES

1. L. Thunus, R. Lejeune, *Coord. Chem. Rev*. **184** (1999) 125 (https://doi.org/10.1016/S0010-8545(98)00206-9)
2. S. J. Coles, M. B. Hursthouse, D. G. Kelly, A. J. Toner, N. M. Walker, *Dalton Trans.* (1998) 3489 (https://doi.org/10.1039/A805764H)
3. A. K. Sharma, S. Chandra, *Spectrochim. Acta, A* **78** (2011) 337 (https://doi.org10.1016/j.saa.2010.10.017)
4. C. A. McAuliffe, R. V. Parish, S. M. Abu-El-Wafa, R. M. Issa, *Inorg. Chim. Acta* **115** (1986) 91 (https://doi.org/10.1016/S0020-1693(00)87702-6)
5. S. Zolezzi, E. Spodine, A. Decinti, *Polyhedron* **21** (2002) 55 (https://doi.org/10.1016/S0277-5387(01)00960-3)
6. V. Ambike, S. Adsule, F. Ahmed, Z. Wang, Z. Afrasiabi, E. Sinn, F. Sarkar, S. Padhye, *J. Inorg. Biochem.* **101** (2007) 1517 (https://doi.org/10.1016/j.jinorgbio.2007.06.028)
7. T. W. Hambley, L. F. Lindoy, J. R. Reimers, P. Turner, W. Wei, A. N. W. Cooper, *Dalton Trans.* (2001) 614 (https://doi.org/10.1039/B008789K)
8. S. Chandra, L. K. Cupta, *Transition Met. Chem*. **30** (2005) 630 (https://doi.org/10.1007/s11243-005-4826-4)
9. G. Y. Nagesh, K. M. Raj, B. H. M. Mruthyunjayaswamy, *J. Mol. Struct*. **1079** (2015) 423 (https://doi.org/10.1016/j.molstruc.2014.09.013)
10. M. Salehi, A. Amoozadeh, A. Salamatmanesh, M. Kubicki, G. Dutkiewicz , S. Samiee, *J. Mol. Struct.* **1091** (2015) 81 (https://doi.org/10.1016/j.molstruc.2015.02.060)
11. S. Shukla, R. S. Srivastava, S. K. Shrivastava, A. Sodhi, P. Kumar, *Med. Chem. Res.* **22** (2013) 1604 (https://doi.org/10.1007/s00044-012-0150-7)
12. M. F. Zaltariov, M. Cazacu, M. Avadanei, S. Shova, M. Balan, N. Vornicu., V. C. Varganici, *Polyhedron* **100** (2015) 121 (https://doi.org/10.1016/j.poly.2015.07.030)
13. E. M. Zayed, M. A. Zayed, *Spectrochim. Acta, A* **143** (2015) 81(https://doi.org/10.1016/j.saa.2015.02.024)
14. T. Rosu, E. Pahontu, C. Maxim, R. Georgescu, N. Stanica, G. L. Almajan, A. Gulea, *Polyhedron* **29** (2010) 757 (https://doi.org/10.1016/j.poly.2009.10.017)
15. J. Rahchamani, M. Behzad, A. Bezaatpour, V. Jahed, G. Dutkiewicz, M. Kubicki, M. Salehi, *Polyhedron* **30** (2011) 2611 (https://doi.org/10.1016/j.poly.2011.07.011)
16. T. Castano, A. Encinas, C. Perez, A. Castro, N. E. Campille, C. Gil, *Bioorg. Med. Chem*. **16** (2008) 6193 (https://doi.org/10.1016/j.bmc.2008.04.036)
17. R. G. Bogle, G. S. Whitley, S. C. Soo, A. P. Johnstone, P. Vallance, *Br. J. Pharmacol*. **111** (1994) 1257 (https://doi.org/10.1111/j.1476-5381.1994.tb14881.x)
18. C. Lee, W. Yang, R. G. Parr, *Phys. Rev., B* **37** (1998) 785 (https://doi.org/10.1103/PhysRevB.37.785)
19. A. D. Becke, *J. Chem. Phys*. **98** (1993) 5648 (https://doi.org/10.1063/1.464913)
20. A. Frisch, A. B. Nielsen, A. J. Holder, *Gauss View User Manual*, Gaussian Inc., Pittsburg, PA, 2001 (https://www.cwu.edu/chemistry/sites/cts.cwu.edu.chemistry/files/documents/Gaussian_09_ReferenceManual.pdf)
21. R. Ditchfield, W. J. Hehre, J. A. Pople, *J. Chem. Phys*. **54** (1971) 724 (https://doi.org/10.1063/1.1674902)
22. *Gaussian 09*, *Revision A. 02*,Gaussian, Inc., Wallingford, CT, 2016 (http://wild.life.nctu.edu.tw/~jsyu/compchem/g09/g09ur/m_citation.htm)

23. R. Dennington II, T. Keith, J. Millam, *GaussView, Version 4.1.2*, Semichem Inc., Shawnee Mission, KS, 2007 (https://aae.wisc.edu/aae637/gauss_9_light/UserGuide9.0.pdf)
24. M. A. Ansari, M. K. Haris, A. K. Aijaz, S. Asfia, *Biol. Med.* **3** (2011) 141 (https://www.sid.ir/En/Journal/ViewPaper.aspx?ID=398130)
25. M. Mishra, K. Tiwari, P. Mourya, M. M. Singh, V. P. Singh, *Polyhedron*.**89** (2015) 29 (https://doi.org/10.1016/j.poly.2015.01.003)
26. G. Y. Nagesh, B. H. M. Mruthyunjayaswamy, *J. Mol. Struct.***1085** (2015) 198 (https://doi.org/10.1016/j.molstruc.2014.12.058)
27. S. Gurunath, M. P. Sathisha, V. Naveen, B. Srinivasa, K. Vidyanand, M*ed. Chem. Res.* **20** (2011) 421 (https://doi.org/10.1007/s00044-010-9330-5)
28. A. B. P. Lever, Inorg*anic Electronic Spectroscopy*, *2nd ed*., Elsevier Sci., Amsterdam, 1984 (http://garfield.library.upenn.edu/classics1992/A1992JQ35000002.pdf)
29. K. Rajendra, A. P. Mishra, *J. Saudi Chem. Soc*.**20** (2016) 12 (https://doi.org/10.1016/j.jscs.2012.06.002)
30. M. Gaber, A. M. Hassanein, A. A. Lotfalla, *J. Mol. Struct*. **875** (2008) 322 (https://doi.org/10.1016/j.molstrcu.2007.05.009)
31. F. A. Cotton, C. Wilkinson, C. A. Murillo, M. Bochmann, A*dvanced Inorganic Chemistry*, 6th ed., Wiley, New York, 1999 (ISBN 0-471-19957-5)
32. M. A. Neelkandan, F. Rusalraj, J. Dharmaraja, S. Johnsonraja, T. Jeyakumar, M. Sankaranarayan Pillai, *Spectrochim. Acta, A* **71** (2008) 1599 (https://doi.org/10.1016/j.saa.2008.06.008)
33. A. M. Gouda, H. A. El-Ghamry, T. M. Bawazeer, T. A. Farghaly, A. N. Abdalla, A. Aslam, *Eur. J. Med. Chem.* **145** (2018) 350 (https://doi.org/10.1016/j.ejmech.2018.01.009)
34. A. A. Abdel Aziz, A. Shawky, M. H. Khalil, *Appl. Organomet. Chem.* **32** (2018) 4404 (https://doi.org/10.1002/aoc.4404)
35. T. Koopmans, *Physica* **1** (1934) 104 (https://doi.org/10.1016/S0031-8914(34)90011-2)
36. M. Rocha, A. Di Santo, J. M. Arias, D. M. Gil, A. Ben Altabef, *Spectrochim. Acta, A* **136** (2015) 635 (https://doi.org/10.1016/j.saa.2014.09.077)
37. K. R. S. Gowda, H. S. B. Naik, B. V. Kumar, C. N. Sudhamani, H. V. Sudeep, T. R. R. Naik, G. Krishnamurthy, *Spectrochim. Acta, A* **105** (2013) 229 (https://doi.org/10.1016/j.saa.2012.12.011)
38. L. P. Nitha, R. Aswathy, N. E. Mathews, B. S. Kumari, K. Mohanan, *Spectrochim. Acta, A* **118** (2014) 154 (https://doi.org/10.1016/j.saa.2013.08.075)
39. K. Mohanan, S. N. Devi, B. Murukan, *Synth. React. Inorg., Met.-Org., Nano-Met. Chem.* **36** (2006) 441 (https://doi.org/10.1080/15533170600777788)
40. T. Arun, S. Packianathan, M. Malarvizhi, R. Antony, N. Raman, *J. Photochem. Photobiol., B* **149** (2015) 93 (https://doi.org/10.1016/j.jphotobiol.2015.05.022)
41. R. Senthil Kumar, S. Arunachalam, *Polyhedron* **26** (2007) 3255 (https://doi.org/10.1016/j.poly.2007.03.001).